

8/22/94

**OBSERVATION OF  $CH A^2\Delta \rightarrow X^2\Pi$ , AND  $B^2\Sigma^- \rightarrow X^2\Pi$ , EMISSIONS  
IN GAS-PHASE COLLISIONS OF FAST  $O(^3P)$  ATOMS WITH ACETYLENE**

**O. J. Orient<sup>1</sup>, A. Chutjian<sup>1</sup>, and E. Murad<sup>2</sup>**

<sup>1</sup> Jet Propulsion Laboratory, California Institute of Technology, Pasadena, CA 91109

<sup>2</sup> Phillips Laboratory/WSCI, 29 Randolph Road, Hanscom AFB, MA 01731-3010

**ABSTRACT**

Optical emissions in single-collision, beam-beam reactions of fast (3-22 eV translational energy)  $O(^3P)$  atoms with  $C_2H_2$  have been measured in the wavelength range 300-850 nm. Two features were observed, one with peak wavelength at 431 nm, corresponding to the  $CH A^2\Delta \rightarrow X^2\Pi$ , transition, and a second weaker emission in the range 380-400 nm corresponding to the  $B^2\Sigma^- \rightarrow X^2\Pi$ , transition. Both the  $A \rightarrow X$  and  $B \rightarrow X$  emissions were fit to a synthetic spectrum of  $CH(A)$  at a vibrational temperature  $T_v$  of 10 000 K (0.86 eV) and a rotational temperature  $T_r$  of approximately 5 000 K (0.43 eV); and  $CH(B)$  to  $T_v = 2 500$  K (0.22 eV) and  $T_r = 1 000$  K (0.09 eV). The energy threshold for the  $A \rightarrow X$  emission was measured to be  $7.3 \pm 0.4$  eV (lab) or  $4.5 \pm 0.2$  eV (c.m.). This agrees with the energy threshold of 7.36 eV (lab) for the reaction  $O(^3P) + C_2H_2 \rightarrow CH(A) + HCO$ .

**PACS CLASSIFICATION NO.: 34.50 Lf**

## I. INTRODUCTION

Studies of low energy atom-molecule collisions are useful in following the transition from endoergic to exoergic chemical reaction as the center-of-mass (c.m.) energy is increased in a controlled fashion. New reaction channels open at the higher energies, and by following emission intensity from a reaction product as a function of c.m. energy, one can identify the open reaction channel. In this paper we report first results of optical emissions following the collision of low energy ( $E_{lab} = 3-22$  eV)  $O(^3P)$  atoms with acetylene under single-collision, crossed-beams conditions. The observed emissions indicate that there is significant conversion of projectile translational energy to internal electronic excitation. Moreover, the absence of emission shows that certain open exit channels can clearly be favored over others. In the present work, one finds significant emission from CH in the  $A^2\Delta$  state, but extremely weak emission from the open  $B^2\Sigma^-$  channel, indicative of small potential in that level, very likely due to a potential barrier towards decay into CH(B). By following the  $A \rightarrow X$  emission intensity as a function of c.m. collision energy, we have also identified the reaction in this energy regime to be  $O(^3P) + C_2H_2(X^1\Sigma_g^+) \rightarrow CH(A^2\Delta) + CHO(X^2A')$ .

## II. EXPERIMENTAL METHODS

The AO source, target region, and spectrometer system used in these

measurements were the same as those used previously in single-collision, beam-beam collision studies of the gaseous targets H<sub>2</sub>O, CO<sub>2</sub> [1], HCN [2], and hydrazines molecules [3]. The retarding-potential difference method (RPD) used herein was also described in Ref. 2. Briefly, the collision measurements are carried out in a uniform, high-intensity (6T) solenoidal magnetic field (see Fig. 1 of Ref. 4). Magnetically-confined electrons of 8.0 eV energy dissociatively attach to a beam of NO to form N + O<sup>-</sup>(<sup>2</sup>P). The magnetically-confined O<sup>-</sup> ions are accelerated to the desired final energy, and are separated from the electrons by a trochoidal deflector. The electrons are photodetached from the O<sup>-</sup> ions using all visible lines from a 20 W argon-ion laser in a multiple-pass geometry. The detachment fraction is 8-15%, depending upon the velocity of the O<sup>-</sup> ions through the detachment region. The resulting O atoms are left exclusively in the ground <sup>3</sup>P state. The O and (undetached) O<sup>-</sup> beams are then directed towards the acetylene target. The O<sup>-</sup> ions and any photodetached electrons are reflected prior to reaching the acetylene beam by a negative bias on the photon-collection mirror upstream of the target.

The RPD method was applied to the magnetically-confined ions by biasing a grid placed before the sample holder, with the sample holder used as a charge collector. The O<sup>-</sup> current on the holder was measured as a function of negative retarding voltage on the grid. This technique measures only the axial energy width of the O<sup>-</sup> beam. The radial energy width is estimated to be about 0.1 eV or less [2]. The O(<sup>3</sup>P) energy distribution was taken from the derivative of the RPD-measured O<sup>-</sup>(<sup>2</sup>P) distribution, with correction for the changing detachment efficiency across the energy bandwidth

[2].

The acetylene beam is formed by effusion through a 1.0 mm-dia. hypodermic needle. The target region was differentially pumped with a cryopump to maintain a pressure difference of  $1.3 \times 10^{-4}$  Pa (source) and  $2.7 \times 10^{-6}$  Pa (target) during operation. Base pressures were  $1 \times 10^{-6}$  Pa and  $7 \times 10^{-8}$  Pa at the source and target, respectively. Optical emissions from the collision region are collected with a spherical mirror and focused onto the entrance plane of a double-grating monochromator. Separate spectra of the emissions and backgrounds are recorded *via* multichannel scaling. The spectral resolution is 4.0 nm [full width at half-maximum (FWHM)]. The principal sources of backgrounds are O<sup>+</sup> collisions with surfaces, and in the wavelength range 450-550 nm scattered light from the argon-ion laser and the directly-heated electron emitter filament.

The acetylene was obtained commercially [5] with a minimum stated purity of 99.6%. It was not purified further. All valves and transfer lines were stainless steel.

### III. EMISSION SPECTRUM AND REACTION THRESHOLDS

#### A. Emission Spectrum

The relation between laboratory (lab) and center-of-mass (c.m.) energies is given by the standard expression [6]

$$E_{CM} = \frac{m_1 m_2}{m_1 + m_2} \left[ \frac{E_1}{m_1} + \frac{E_2}{m_2} - 2 \left( \frac{E_1 E_2}{m_1 m_2} \right)^{1/2} \cos \theta \right] \quad (1)$$

where  $m_i$  and  $E_i$  are masses and laboratory energies (subscripts 1,2 refer to O and the acetylene molecule, respectively). The energy of the acetylene beam is thermal ( $E_2 = 0.04$  eV), and the angle  $\theta$  between the AO and molecular beams is centered at  $90^\circ$  for crossed-beams collisions, with a total angular width  $2\Delta\theta$  estimated to be at most  $20^\circ$ . Contribution from the second term in Eq. (1) (order of 0.01 eV c.m. energy) is neglected, as is the effect (third term, order of 0.01 eV c.m. energy) of the  $2\Delta\theta$  width. The second and third terms are also of opposite sign and cancel at the  $10^{-3}$  eV level. In this case Eq.(1) reduces to  $E_{c.m.} = 0.619 E_1$ . Equation (1) is based only upon the laboratory energies of the incident particles, and gives no information on the energy sharing between the outgoing particles in the given reaction channel.

The emission spectrum of the  $O(^3P) + C_2H_2$  system is shown in Fig. 1 at a c.m. energy of 8.7 eV. The prominent feature peaking at 431 nm corresponds to the  $A^2\Delta \rightarrow X^2\Pi$ , emission, while the much weaker emission in the range 380-400 nm is the  $B^2\Sigma^- \rightarrow X^2\Pi$ , transition [7]. No other emissions in the range 300-850 nm were detected within present instrument sensitivity.

Simulation of the relative emission intensity within each band system, for particular vibrational ( $T_v$ ) and rotational ( $T_r$ ) was carried out using a line-fitting program written in our laboratory [3]. The spectroscopic constants for CH(A) and CH(B) were taken from Ref. 7, Franck-Condon factors from Liszt and Smith [8], and rotational line strengths from Kovacs [9]. The calculated emission spectrum was convoluted with a Gaussian slit function of 4.0 nm (FWHM). Results of the fittings for the  $A \rightarrow X$  and  $B \rightarrow X$  emissions are indicated in Fig. 1. From a visual estimate, the

derived temperatures were, for the  $A \rightarrow X$  system,  $T_v = 10\ 000\ \text{K}$ ,  $T_r = 5\ 000\ \text{K}$ ; and for the  $B \rightarrow X$  system,  $T_v = 2\ 500\ \text{K}$ ,  $T_r = 1\ 000\ \text{K}$ . The fittings are relatively insensitive to the rotation temperatures, since the ratio of rotational B-value to optical resolution is small ( $15\ \text{cm}^{-1}/250\ \text{cm}^{-1}$ ).

In the case of  $\text{O}(^3\text{P})$  reaction with the monomethylhydrazine [3] no  $B \rightarrow X$  was detected, even though the  $A \rightarrow X$  emission was prominent. If the  $A$  and  $B$  states were populated equally, the  $B \rightarrow X$  transition should have been about half as intense  $A \rightarrow X$  emission. In the present reaction with acetylene, the intensity of the  $B \rightarrow X$  emission is barely above the minimum detectable. No explanation for this phenomenon can be given, other than that a potential barrier may exist in this collision system towards decay to the  $\text{CH}(B)$  state.

### B. Reaction Threshold

The RPD spectrum is shown in Fig. 2. Here, the monochromator wavelengths was fixed at 431 nm (peak of the  $A \rightarrow X$  emission), and the emission intensity monitored as a function of  $\text{O}(^3\text{P})$  energy. After unfolding the effects of the  $\text{O}(^3\text{P})$  energy distribution, one obtains a threshold energy of  $7.3 \pm 0.4\ \text{eV}$  (lab) or  $4.5 \pm 0.2\ \text{eV}$  (c.m.). As noted in Ref. 2 this threshold is likely an upper limit, since it includes additional vibrational, rotational, and translational energy in the  $\text{CH} +$  fragments; and thresholds often trend towards lower energies with increases in measurement sensitivity.

In order to identify the reaction involved, we list in Table I the enthalpies of possible reactions which can produce excited  $\text{CH}$ . Thermochemical data were taken

from Ref. 10, and the supporting data used are given in Table II. The threshold results of Fig. 2 clearly point to Reaction 4 as the reaction channel. A similar measurement could not be made for the  $B \rightarrow X$  emission due to poor signal-to-background ratio. However, the fact that this channel is open at 8.7 eV c.m. energy (Fig. 1) is consistent with Reaction 5 (threshold at 7.86 eV) as the principal channel.

### **ACKNOWLEDGEMENTS**

This work was carried out at the Jet Propulsion Laboratory, California Institute of Technology and the Air Force Phillips Laboratory. It was supported by the AFOSR and the Phillips Laboratory through agreement with the National Aeronautics and Space Administration.

## REFERENCES

- [1] O.J. Orient, A. Chutjian and E. Murad, *Phys. Rev. Lett.* **65**, 2359 (1990).
- [2] O. J. Orient, A. Chutjian, K. E. Martus and E. Murad, *Phys. Rev. A* **48**, 427 (1993).
- [3] O.J. Orient, A. Chutjian and E. Murad, *J. Chem. Phys.* **00**, 0000 (1994).
- [4] O. J. Orient, K. E. Martus, A. Chutjian and E. Murad, *Phys. Rev. A* **45**, 2998 (1992).
- [5] source of acetylene
- [6] K.T. Dolder and B. Peart, *Rep. Prog. Phys.* **39**, 693 (1976).
- [7] K.P. Huber and G. Herzberg, *Molecular Spectra and Molecular Structure IV. Constants of Diatomic Molecules* (Van Nostrand Reinhold, New York 1979), p. 154 (CN).
- [8] H. S. Liszt and W. H. Smith, *J. Quant. Spectr. Rad. Transfer* **12**, 947 (1972).
- [9] I. Kovacs, *Rotational Structure in the Spectra of Diatomic Molecules* (American Elsevier, New York, 1969) Ch. 3.
- [10] S. E. Stein, *NIST Standard Reference Database No. 25, NIST Structures and Properties* (available on disk from NIST, Gaithersburg MD 20899).

**Table I. Threshold energies in the center-of-mass (c.m.) and laboratory (lab) frames for reactions of O(<sup>3</sup>P) and acetylene. Possible emitting species are indicated in bold type.**

Reaction Number	Reaction	Threshold Energy (eV)	
		c.m.	lab
1	$O(^3P) + C_2H_2(X^1\Sigma_g^+) \rightarrow C_2(X^1\Sigma_g^+) + H_2O(X^1A_1)$	1.17	1.89
2	$O(^3P) + C_2H_2(X^1\Sigma_g^+) \rightarrow CH_2(X^3\Sigma_g^-) + CO(X^1\Sigma^+)$	-2.06	-3.33
3	$O(^3P) + C_2H_2(X^1\Sigma_g^+) \rightarrow CH(X^2\Pi_r) + CHO(X^2A')$	1.68	2.71
4	$O(^3P) + C_2H_2(X^1\Sigma_g^+) \rightarrow CH(A^2\Delta) + CHO(X^2A')$	4.56	7.36
5	$O(^3P) + C_2H_2(X^1\Sigma_g^+) \rightarrow CH(B^2\Sigma^-) + CHO(X^2A')$	4.87	7.86
6	$O(^3P) + C_2H_2(X^1\Sigma_g^+) \rightarrow CH(X^2\Pi_r) + CHO(A^2A')$	2.83	4.58
7	$O(^3P) + C_2H_2(X^1\Sigma_g^+) \rightarrow C_2O(X^3\Sigma) + H_2(X^1\Sigma_g^+)$	-1.98	-3.20
8	$O(^3P) + C_2H_2(X^1\Sigma_g^+) \rightarrow OH(X^2\Pi_r) + C_2H(X^2\Sigma)$	1.31	2.12
9	$O(^3P) + C_2H_2(X^1\Sigma_g^+) \rightarrow OH(A^2\Sigma^+) + C_2H(X^2\Sigma)$	5.33	8.60

**Table II.** Auxiliary thermodynamic data. All heats of formation are taken from the compilation by Stein [10]. Conversion to the eV scale is 23.06 kcal/mole = 1 eV.

Species	$\Delta H_f(g, 298 \text{ K}), \text{ kcal/mol}$
O( $^3P$ )	+59.6
C <sub>2</sub> H <sub>2</sub> (X $^1\Sigma_g^+$ )	+54.5
CH(X $^2\Pi_r$ )	+142.4
CH(A $^2\Delta$ )	+208.8
CH(B $^2\Sigma^-$ )	+215.9
OH(X $^2\Pi_r$ )	+9.3
C <sub>2</sub> (X $^1\Sigma_g^+$ )	+198.8
C <sub>2</sub> H(X $^2\Sigma$ )	+135.0
C <sub>2</sub> O(X $^3\Sigma$ )	+68.4
CH <sub>2</sub> (X $^3\Sigma_g^-$ )	+93.0
CHO(X $^2A'$ )	+10.4
CHO(A $^2A''$ )	+68.4
CO(X $^1\Sigma^+$ )	-26.4
H <sub>2</sub> O(X $^1A_1$ )	-57.8
H <sub>2</sub> (X $^1\Sigma_g^+$ )	0.0

## FIGURE CAPTIONS

### Figure 1

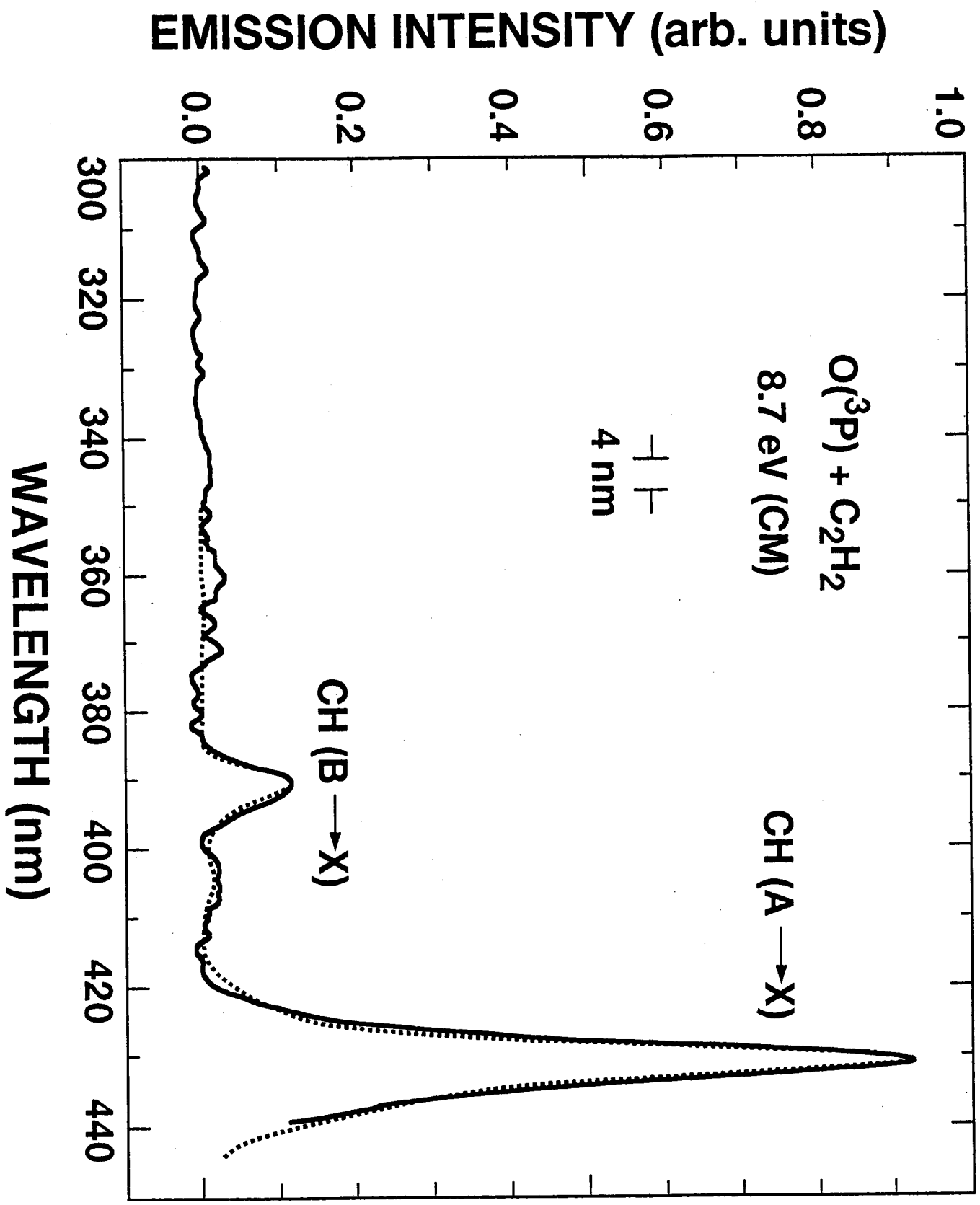
Measured ( — ) and simulated ( ■■■■ ) spectrum of the  $CH A^2\Delta \rightarrow X^2\Pi$ , and  $CH B^2\Sigma^- \rightarrow X^2\Pi$ , emission systems at 8.7-eV c.m. energy. The simulations correspond to vibrational and rotational temperatures of  $T_v = 10\,000$  K (0.86 eV) and  $T_r = 5\,000$  K (0.43 eV), respectively, for the  $A$  state; and  $T_v = 2\,500$  K (0.22 eV) and  $T_r = 1\,000$  K (0.09 eV), respectively, for the  $B$  state.

### Figure 2

Energy distribution of the  $O(^2P)$  ions at an ion current of  $10.8\ \mu\text{A}$  as obtained from retarding potential difference (RPD) measurements. Shown are the  $O^-$  and the  $O(^3P)$  distributions, the latter obtained from the derivative of the RPD curve, corrected for the variation with  $O^-$  velocity of detachment efficiency across the line width. The peak  $O(^3P)$  energy here is  $12.0 \pm 0.2$  eV and the FWHM is  $1.2 \pm 0.1$  eV.

### Figure 3

Excitation of the  $A \rightarrow X$  emission at 431 nm as a function of  $O(^3P)$  lab energy in the range 3-21 eV (curve A). The excitation function has been deconvoluted from the energy distribution of the  $O(^3P)$  atoms (1.2 eV FWHM here; see also Fig. 3 of Ref. 2). The excitation threshold is measured to be  $7.3 \pm 0.4$  eV (lab, as measured from the  $A \times 3$  curve). Dotted portion at threshold (●●●) is the intensity without deconvolution, showing effects of a high-energy tail in the  $O(^3P)$  energy distribution. Threshold for Reaction 4 (Table I) is indicated by arrow.



# PARTICLE CURRENT (arb. units)

